Spectrochimica Acta Part A 78 (2011) 503–511

Contents lists available at ScienceDirect

Spectrochimica Acta Part A: Molecular and Biomolecular Spectroscopy

journal homepage: www.elsevier.com/locate/saa

Spectroscopic studies on the interaction between Pr(III) complex of an ofloxacin derivative and bovine serum albumin or DNA

Min Xu, Zhao-Rong Ma, Liang Huang, Feng-Juan Chen, Zheng-zhi Zeng*

Key Laboratory of Nonferrous Metals Chemistry and Resources Utilization of Gansu Province, State Key Laboratory of Applied Organic Chemistry and College of Chemistry and Chemical Engineering, Lanzhou University, Lanzhou 730000, PR China

ARTICLE INFO

Article history:
Received 31 July 2010
Received in revised form 12 October 2010
Accepted 15 November 2010

Keywords:
Pr(III) complex
Bovine serum albumin
Calf thymus DNA
pBR 322 DNA

ABSTRACT

The binding properties on $[PrL_2(NO_3)](NO_3)_2$ (L = 9-fluoro-2,3-dihydro-3-methyl-10-(4-methyl-1-piperaziny)-7-oxo-7Hpyrido[1,2,3-de]-1,4-benzoxazine-6-carbaldehyde benzoyl hydrazone) to bovine serum albumin (BSA) have been studied for the first time using fluorescence spectroscopy in combination with UV–Vis absorbance spectroscopy. The results showed that $[PrL_2(NO_3)](NO_3)_2$ strongly quenched the intrinsic fluorescence of BSA through a static quenching procedure, and non-radiation energy transfer happened within molecules. The number of binding site was about 1, and the efficiency of Förster energy transfer provided a distance of 4.26 nm between tryptophan and $[PrL_2(NO_3)](NO_3)_2$ binding site. At 288, 298, 310 K, the quenching constants of BSA–$[PrL_2(NO_3)](NO_3)_2$ system were 5.11×10^4, 4.33×10^4 and $3.71 \times 10^4\,l\,M^{-1}$. ΔH, ΔS and ΔG were obtained based on the quenching constants and thermodynamic theory ($\Delta H < 0$, $\Delta S > 0$ and $\Delta G < 0$). These results indicated that hydrophobic and electrostatic interactions are the mainly binding forces in the $[PrL_2(NO_3)](NO_3)_2$–BSA system. In addition, the CD spectra have proved that BSA secondary structure changed in the presence of $[PrL_2(NO_3)](NO_3)_2$ in aqueous solution. Moreover, the interaction between $[PrL_2(NO_3)](NO_3)_2$ and calf thymus DNA (CT DNA) was studied by spectroscopy and viscosity measurements, which showed that the binding mode of the $[PrL_2(NO_3)](NO_3)_2$ with DNA is intercalation. The DNA cleavage results show that in the absence of any reducing agent, the $[PrL_2(NO_3)](NO_3)_2$ can cleave plasmid pBR322 DNA and its hydrolytic mechanism was demonstrated with hydroxyl radical scavengers and singlet oxygen quenchers.

1. Introduction

In the past years, many studies on the molecular structure of metal complexes and their biological activity caused much interest in the field of inorganic chemistry [1,2]. Serum albumin as one of the most abundant carrier proteins plays an important role in the transport and disposition of endogenous and exogenous ligands present in blood [3]. The nature and magnitude of drug–albumin interactions significantly influence the pharmacokinetics of drugs, and the binding parameters are useful in studying protein–drug binding as they greatly influence absorption, distribution, metabolism, and excretion properties of typical drugs [4]. Furthermore, DNA is an important cellular receptor, many chemicals exert their antitumor effects through binding to DNA thereby changing the replication of DNA and inhibiting the growth of the tumor cell, which is the basis of designing new and more efficient antitumor drugs and their effectiveness depends on the mode and affinity of the binding [5–7]. Therefore, this inspires considerable interest in the study of the biochemical behavior of some compounds including their interactions with serum proteins and DNA, which are primary target molecules, when metal compound is administered intravenously [8–12].

Ofloxacin (OFLX, (±) 9-fluoro-2,3-dihydro-3-methyl-10-(4-methyl-1-piperaziny)-7-oxo-7H-pyrido[1,2,3-de]-1,4-benzoxazine-6-carboxylic acid, Fig. 1) is one of the most frequently used fluorinated quinolones antibiotics in the world [13]. It has a broad spectrum of activity against gram-positive, gram-negative aerobic, facultatively anaerobic bacteria, chlamydiae, and some related organisms, such as mycoplasmas or mycobacteria [14]. Several transition metal complexes of quinolones antibiotics have been synthesized, characterized and evaluated for various biological activities [15–17]. However, studies on biological activities of the rare earth metal complexes with ofloxacin derivative have been rarely reported.

Based on the above consideration, we synthesized and characterized a novel ligand derivated from ofloxacin and its Pr(III) complex. The interactions of BSA with Pr(III) complex have been studied by using spectroscopy under simulative physiological conditions. The quenching mechanism of fluorescence of BSA by Pr(III) complex was explored by fluorescence spectrum at different temperatures and UV–Vis spectrum. The number of binding site and

* Corresponding author. Tel.: +86 931 8912582; fax: +86 931 8912582.
E-mail address: zengzhzh@yahoo.com.cn (Z.-z. Zeng).

1386-1425/$ – see front matter © 2010 Elsevier B.V. All rights reserved.
doi:10.1016/j.saa.2010.11.018

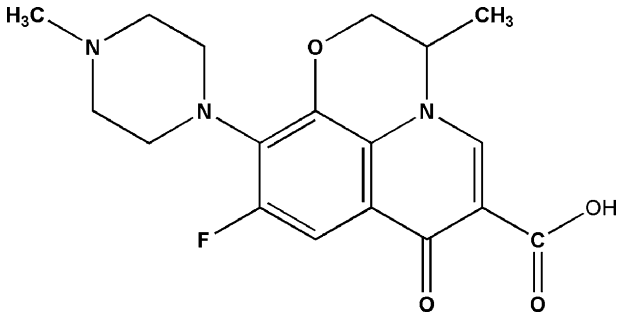

Fig. 1. The structure of ofloxacin.

main sort of binding force in the medium of Tris–HCl buffer solution (pH 7.4) have been suggested. In addition, according to the mechanism of Förster's theory, the transfer efficiency of energy and distance between the acceptor BSA and the donor Pr(III) complex were calculated. Moreover, to explore the conformational changes of BSA during the course of binding, we employed CD, a well-known spectroscopic technique for obtaining information on the secondary structure of proteins [18,19], together with methods (SELCON3, CONTIN, CDSSTR) for estimating protein secondary structures from CD spectra [20–23]. The assignments obtained from these methods gave six types of secondary structures: regular α-helix, α_R; distorted α-helix, α_D; regular β-strand, β_R; distorted β-strand, β_D; turns, T; and unordered, U. The results suggest that the Pr(III) complex influence the secondary structure of BSA. Meanwhile, we described a comparative study of the interaction of Pr(III) complex and the ligand with CT DNA using spectroscopy and viscosity measurements. Furthermore, this Pr(III) complex was found to cleave pBR 322 DNA at physiological pH and temperature.

2. Experimental

2.1. Materials

All chemicals were purchased from commercial sources, and used as received without further purification. CT-DNA and pBR322 DNA were obtained from Sigma–Aldrich (USA). Agarose was purchased from Promega (German). EB and other chemicals were local products of analytical grade. Solutions of CT-DNA in 50 mM NaCl, 5 mM Tris–HCl (tris(hydroxymethyl)aminomethane hydrochloride) (pH 7.2) gave a ratio of UV–Vis absorbance of 1.8–1.9:1 at 260 and 280 nm, indicating that the DNA was sufficiently free of protein [24]. The CT-DNA concentration per nucleotide was determined spectrophotometrically by employing an extinction coefficient of 6600 M^{-1} cm^{-1} at 260 nm. Stock solution of CT-DNA was stored at 277 K and used after no more than 4 days.

2.2. Physical measurements

The melting points of the compounds were measured on a Beijing XT4-100× microscopic melting point apparatus (the thermometer was not corrected). Elemental analysis was carried out by using an Elemental Vario EL analyzer. Infrared spectra (4000–400 cm^{-1}) were recorded with KBr disks by using a Therrno Mattson FTIR spectrometer. The UV–Vis spectra were recorded on a Varian Cary 100 Conc spectrophotometer. ^{1}H NMR spectra were measured on a Varian VR 400-MHz spectrometer by using TMS as a reference in DMSO-d^6. Mass spectra were measured on aVGZAB-HS (FAB) instrument. The fluorescence spectra were recorded on a Hitachi RF-4500 spectrofluorophotometer.

2.3. Procedure

2.3.1. Preparation of the ligand

The ligand (Fig. 2) was prepared according to a modified method of the literature [25]. Ofloxacin (18.82 g; 50 mmol) was esterified to 9-fluoro-2,3-dihydro-3-methyl-10-(4-methyl-1-piperaziny)-7-oxo-7H-pyrido [1,2,3-de]-1,4-benzoxazine-6-carboxylate, treatments of the esters with $N_2H_4{\cdot}H_2O$ gave the corresponding hydrazine (18.19 g; (86%)), which was refluxed 3 h mixed with 2,4-dihydroxybenzaldehyde, the ligand was obtained in 84% yield.

Ester: white solid, m.p. 238–240 °C, ^{1}H NMR (CD_3OH, 400 MHz) δ (ppm): 1.432–1.449 (3H, d, J = 6.8 Hz, –CH_3), 2.361–2.375(3H, d, J = 5.6 Hz, –N–CH_3), 2.642 (4H, s, 1′,4′-H), 3.230–3.238(1H, m, 2-H), 3.325–3.336(4H, d, 2′,3′-H), 4.331–4.535(2H, m, 1-H), 7.360–7.391(1H, d, 3-H), 8.511(1H, s, 7-H).

Hydrazine: yellowish solid, m.p. 200–202 °C, ^{1}H NMR (CD_3OH, 400 MHz) δ (ppm): 1.462–1.478 (3H, d, J = 6.4 Hz, –CH_3), 2.290(3H, s, –N–CH_3), 2.526 (4H, s, 1′,4′-H), 3.229–3.236 (1H, m, 2-H), 3.261–3.333 (4H, d, 2′,3′-H), 4.289–4.444 (2H, m, 1-H), 7.305–7.336 (1H, d, 3-H), 8.559 (1H, s, 7-H).

Ligand: $C_{25}H_{26}FN_5O_5$, white solid, m.p. 264–266 °C, ^{1}H NMR (DMSO-d^6, 200 MHz) δ (ppm): 1.703–1.733(3H, d, J = 6.0 Hz, –CH_3), 2.507–2.781 (7H, m, –N–CH_3, 1′,4′-H), 3.443–3.628 (5H, m, 2-H, 2′, 3′-H), 4.396–4.665 (2H, m, 1-H), 4.811–5.201 (2H, s, –OH, –OH), 7.099–7.138 (2H, d, 1′, 3′-H), 7.786 (1H, s, 7-H), 8.550 (1H, s, 4′-H), 9.157 (1H, s, 3-H), 10.215 (1H, s, –CH=N). FAB-MS: m/z = 496.1 $[M+H]^+$. Anal. Calcd for $C_{25}H_{26}FN_5O_5$: C, 60.62; H, 5.32; N, 14.16. Found: C, 60.60; H, 5.29; N, 14.13. IR ν_{max} (cm^{-1}): ν(N–H):3352, ν(hydrazonic)C=O: 1658, ν(C=N): 1608. UV: λ_{max} (nm): 300, 356.

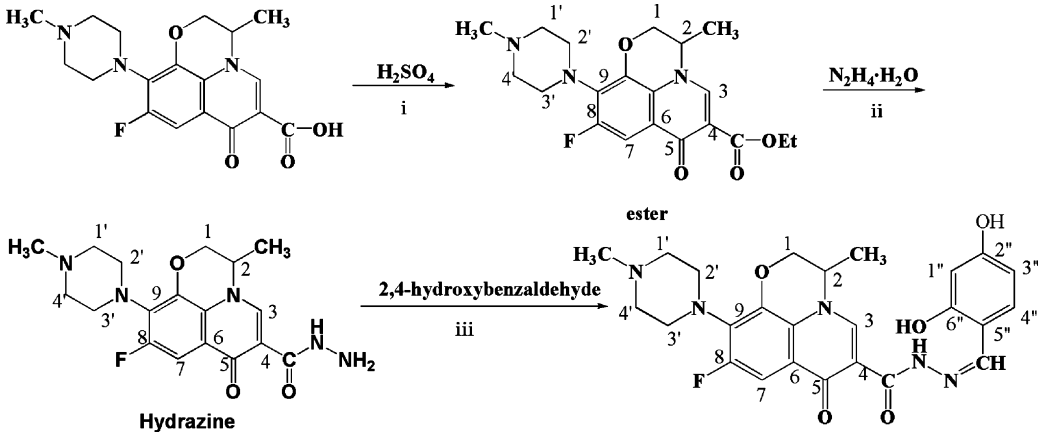

Fig. 2. The synthetic route of the ligand: (i) C_2H_5OH, reflux, 20 h; (ii) C_2H_5OH, reflux, 4 h; (iii) CH_3OH, reflux, 3 h.

2.3.2. Preparation of the complex

Ligand (0.119 g, 0.25 mmol) and NaOH (0.01 g, 0.25 mmol) was mixed in 15 ml CH_3OH, which stirred for 0.5 h at 60 °C, then $Pr(NO_3)_3{\cdot}6H_2O$ (0.1299 g, 0.3 mmol) was added to the yellowish solution. The solution turned to deep yellow immediately and further stirred 3 h at room temperature. A yellow precipitate, the Pr(III) complex was separated from the solution by suction filtration, purified by washing several times with methanol, and dried for 24 h under vacuum. Yield: 65%. Anal. Calcd for $C_{50}H_{52}F_2N_{13}O_{19}Pr$: C, 45.60; H, 3.99; N, 13.84. Found: C, 45.56; H, 3.95; N, 13.82. IR ν_{max} (cm^{-1}): ν(N–H): 3373, ν(C=O): 1621, ν(C=N): 1587, $\nu(NO_3)$: 1476, UV: λ_{max} (nm): 305, 363. λm ($S\,cm^2\,M^{-1}$): 146.8.

2.3.3. BSA binding experiments

The protein-binding study was performed by fluorescence quenching experiments using BSA, 3 μM in Tris–HCl buffer (pH 7.4). The quenching of the emission intensity of BSA at 341 nm was monitored using complexes as quenchers with increasing concentration. Fluorescence spectra were recorded from 300 to 500 nm at an excitation wavelength of 280 nm. The experiments were measured at three temperatures (288, 298 and 310 K). The temperature of sample was kept by recycled water throughout the experiment. Fluorescence spectrum scan was recorded at room temperature and similar in methods to titration experiments.

A Varian Carry 100UV–Vis spectrophotometer equipped with 1.0 cm quartz cells was used for scanning the UV spectrum on the range of wavelength from 190 to 400 nm. The Tris/HCl buffer solution was used as a reference solution.

Circular dichroism (CD) measurements were made on an Olis RSM 1000 CD spectrometer in cell of 1 mm path length at room temperature. CD spectra (200–260 nm) were taken at a BSA concentration of 1.50×10^{-6} M, and the results were taken as molar absorbance ([$\Delta\varepsilon$]) in $cm^2\,dM^{-1}$. In order to obtain the secondary structure fractions of BSA, the CDPro software package was used. This consists of the three programs, SELCON3, CONTIN, and CDSSTR, and a program for determining tertiary structure class (CLUSTER). One of the major advantages of the CDPro software package is that the programs have been modified to accept any given set of reference proteins (CD spectra and secondary structure fractions), and seven such reference sets are provided. Moreover, input data files for these three programs are identical. More information about CDPro is available at the following website: http://lamar.colostate.edu/sreeram/CDPro [26].

2.3.4. DNA binding experiments

The interaction of complexes with CT DNA has been studied with UV spectroscopy in order to investigate the possible binding modes to CT DNA and to calculate the binding constants to CT DNA (K_b). In UV titration experiments, the spectra of CT DNA in the presence of each complex have been recorded for a constant CT DNA concentration in diverse [complex]/[CT DNA] mixing ratios (r).

The competitive studies of each compound with EB have been investigated with fluorescence spectroscopy in order to examine whether it is able to displace EB from its CT DNA–EB complex. The CT DNA–EB complex was prepared by adding 0.32 μM EB and 4 μM CT DNA in Tris–HCl buffer (pH 7.2). The intercalating effect of compounds with the DNA–EB complex was studied by adding a certain amount of a solution of the compound step by step into the solution of the DNA–EB complex. The influence of the addition of each compound to the DNA–EB complex solution has been obtained by recording the variation of fluorescence emission spectra.

Iodide quenching experiments were used potassium iodide as the quencher to determine the relative accessibilities of the free and bound the Pr(III) complex.

The effect of the ionic strength on the compounds was also investigated with fluorescence spectroscopy. Fluorescence intensities were recorded in the absence and presence of DNA in the mixture solution of each compound and NaCl at room temperature.

Viscosity experiments were conducted on an Ubbdlodhe viscometer, immersed in a thermostated water-bath maintained to 25.0 °C. Titrations were performed for the complexes (1–5 μM), and each compound was introduced into DNA solution (5 μM) present in the viscometer. Data were presented as $(\eta/\eta_c)^{1/3}$ versus the ratio of the concentration of the compound and DNA, where η is the viscosity of DNA in the presence of compound and η_0 is the viscosity of DNA alone. Viscosity values were calculated from the observed flow time of DNA containing solution corrected from the flow time of buffer alone (t_0), $\eta = t - t_0$ [27,28].

2.3.5. DNA cleavage

The cleavage reactions were performed incubating pBR 322 (12 μM base pairs) at 37 °C in the presence/absence of increasing amounts of metal complex for 5 h in TBE buffer [0.045 M tris(hydroxymethyl)aminomethane (tris), 0.045 M boric acid, and 1 mM EDTA, pH 8.3]. And then the samples were analyzed by electrophoresis for 1 h at 100 V on a 0.8% agarose gel in TBE buffer. The gel was stained with 1 mg/ml ethidium bromide and photographed on an Alpha Innotech IS-5500 fluorescence chemiluminescence and visible imaging system.

3. Results and discussion

3.1. Structure of the Pr(III) complexes

The complex is air-stable for extended periods and very soluble in DMSO and DMF; soluble in water, slightly soluble in ethanol and methanol; insoluble in benzene and diethyl ether. The molar conductivity of the complex is 146.8 $S\,cm^2\,M^{-1}$ in DMF solution, showing that this complex is 2:1 electrolytes [29]. The elemental analyses and molar conductivities show that formulas of the Pr(III) complex conform to $[PrL_2(NO_3)](NO_3)_2$.

3.1.1. Infrared spectrum study

IR spectra usually provide a lot of valuable information on coordination reactions. All the spectra are characterized by vibrational bands mainly due to the NH, C=O, C=N and NO_3 groups. The ν(N–H) appears at 3352 cm^{-1} for the ligand, and this peak shifts at 3373 cm^{-1} or so for the Pr(III) complex. The ν(C=O) vibration of the free ligand is at 1658 cm^{-1}; for the Pr(III) complex, the peak shifts to 1621 cm^{-1}, $\Delta\nu$(ligand–complexes) is equal to 37 cm^{-1}. In the complex, the band at 585 cm^{-1} or so is assigned to ν(M–O). It demonstrates that the oxygen of carbonyl has formed a coordinative bond with the lanthanide ions [30]. The band at 1608^{-1} cm for the free ligand is assigned to the ν (C=N) stretch, which shifts to 1587 cm^{-1} for its Pr(III) complex, $\Delta\nu$ (ligand–complexes) is equal to 21 cm^{-1}. Weak bands at 410 cm^{-1} or so are assigned to ν (M–N) in the complex. These shifts and new bands further confirm that the nitrogen of the imino-group bonds to the Pr(III) ions [31]. The absorption bands of the coordinated nitrates were observed at about 1476 (ν_{as}) and 855 (ν_s) cm^{-1}. The ν3 free nitrates appear at 1384 cm^{-1} or so in the spectra of the Pr(III) complexes. In addition, the separation of the two highest frequency bands $|\nu_4 - \nu_1|$ is approximately 160 cm^{-1}, and accordingly the coordinated NO_3^- ion in the complex is a bidentate ligand [32].

3.1.2. Thermal studies

The thermogravimetric analysis of the complexes have been carried out in nitrogen environment over the temperature range 30–1200 °C. The complexes begin to decompose at 300 °C or so and there are two exothermic peaks appear around 300–564 °C. The corresponding TG curves show a series of weight loss. Under 200 °C,

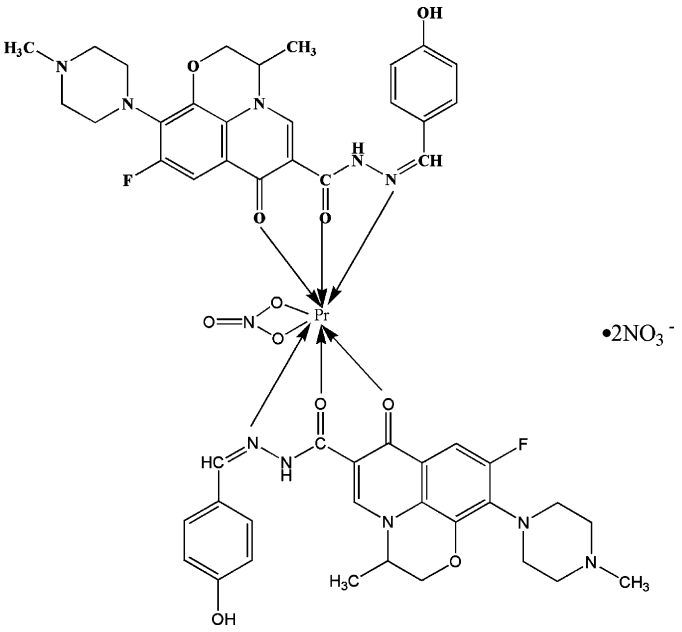

Fig. 3. The suggested structure of $[PrL_2(NO_3)](NO_3)_2$.

there are no endothermic peaks and no weight loss on the corresponding curves. It indicates that there are no crystal or coordinate solvent molecules. While being heated to 800 °C, the curve became plateau because complexes become their corresponding oxides.

3.1.3. UV spectra

The UV–Vis absorption spectra of the investigated compounds in the absence and in the presence of the CT-DNA were obtained in DMF:Tris–HCl buffer (pH 7.20) containing 50 mmol NaCl of 1:100 solutions, respectively. The UV–Vis spectra of ligands have two types of absorption bands at λ_{max} in the regions of 294–302 nm and 352–359 nm, which can be assigned to π–π^* transitions within the organic molecules, and π–π^* of the C=N and C=O groups, respectively. While the UV–Vis spectra of its Pr(III) complex has two types of absorption bands at λ_{max} in the regions of 300–308 nm and 356–365 nm, which can be, respectively, assigned to π–π^* transitions of the larger conjugated organic molecules and π–π^* of the charge transfers from ligands to metal ions ($L \rightarrow Pr^{3+}$) [33,34]. The band shifts of λ_{max} and the changes of ε for complex in comparison with ligand indicate the formations of the complexes.

Since the crystal structures of its Pr(III) complexes have not been obtained yet, we characterized the complexes and determined its possible structure by elemental analyses, molar conductivities, IR spectra, TG/DTA and UV–Vis spectra. The ligand and the Pr(III) ions can form mononuclear ten-coordination $[PrL_2(NO_3)](NO_3)_2$ complex with 1:2 metal-to-ligand stoichiometry at the Pr(III) centers (Fig. 3).

3.2. BSA binding studies

3.2.1. The quenching mechanism of fluorescence of BSA by Pr(III) complex

BSA solutions exhibit a strong fluorescence emission with a peak at 341 nm when excited at 280 nm [35]. An excitation wavelength of 280 nm would excite both tyrosine and tryptophan side chains in proteins, with the overall fluorescence intensity depending, in part, on their relative abundances in the protein [36]. Under the same experiment condition, the fluorescence intensity of its Pr(III) complex was very weak. Addition of the Pr(III) complex to BSA causes a concentration-dependent quenching (Fig. 4).

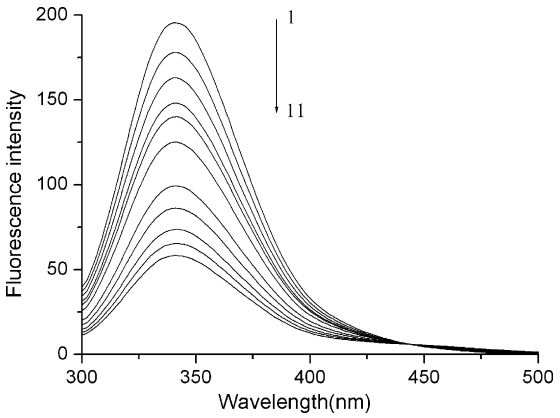

Fig. 4. Fluorescence spectra of BSA–Pr(III) complex system. 1–11 respectively, 1.5×10^{-6} M BSA in the presence of 0.00, 1.25, 3.75, 6.25, 8.75, 12.5, 18.8, 25.0, 31.3, 37.5, 43.8×10^{-6} M Pr(III) complex.

The Stern–Volmer and Lineweaver–Burk graphs may be used in order to study the interaction of a quencher in presence of BSA (see Supporting Information Fig. S1). The curves have fine linear relationship according to Stern–Volmer quenching equation (Eq. (1)) [37].

$$\frac{F_0}{F} = 1 + K_q\tau_0[Q] = 1 + K_{SV}[Q] \quad (1)$$

where F_0 and F are the fluorescence intensity in the absence and presence of the quencher, [Q] is the concentration of the quencher, τ_0 is the average bimolecular lifetime in the absence of quencher and K_q is the bimolecular quenching rate constant which is expected to be proportional to the diffusion coefficients and so to be proportional to the solvent temperature. K_{SV} is the Stern–Volmer quenching constant.

Taking as fluorescence lifetime (τ_0) of BSA at around 10^{-8} s [38], the dynamic quenching constant (K_{SV}, M^{-1}), and subsequently the approximate quenching constant (K_q, $M^{-1}\,s^{-1}$), can be obtained by the slope of the diagram. The calculated values of K_{SV} and K_q for the interaction of the Pr(III) complex with BSA are given in Table 1. Usually, the maximum quenching rate constant of diffusion collision of various quenchers for the biomacromolecule is about $2.0 \times 10^{10}\,M^{-1}\,s^{-1}$ [39]. Obviously, the derived quenching rate constants (which were about $10 \times 10^{12}\,M^{-1}\,s^{-1}$) were higher than the K_q of the diffusion course by two orders of magnitude for complexes. Thus, the fluorescence quenching was the consequence of the static quenching instead of the dynamic collision quenching. Meanwhile, in this study the K_{SV} were found to decrease with an increase in temperature, indicating that static quenching actually occurred in the quenching process [40,41].

To further reveal the nature of quenching, fluorescence lifetime measurements were carried out by using TCSPC technique. Fluorescence lifetime serves as a sensitive parameter for exploring the local environment around a fluorophore, and it is sensitive to excited-state interactions [42]. It also contributes to the understanding of the interactions between the probes and the proteins [43]. The results show that no observed change in the magnitude of

Table 1
The quenching and dissociation constants of BSA with $[PrL_2(NO_3)](NO_3)_2$ at different temperatures.

T (K)	K_q ($\times 10^{12}\,M^{-1}\,s^{-1}$)	K_{SV} ($\times 10^4\,M^{-1}$)	R^2
288	5.11	5.11	0.998
298	4.33	4.33	0.996
310	3.71	3.71	0.996

Table 2
Binding constants K_A, number of binding sites n and thermodynamic parameters for $[PrL_2(NO_3)](NO_3)_2$–BSA.

T (K)	K_A ($\times 10^4$ M^{-1})	n	R^2	ΔG (kJ mol^{-1})	ΔH (kJ mol^{-1})	ΔS (J mol^{-1} K^{-1})
288	5.40	0.911	0.994	−26.08	−16.72	32.50
298	4.21	0.884	0.999	−26.41		
310	3.29	0.912	0.999	−26.80		

the fluorescence lifetime of BSA with the addition of Pr(III) complex was made [44].

The above results obtained both from the steady state and time resolved spectroscopic measurements hint to the occurrence of static-type fluorescence quenching phenomena caused by ground state complex formations between BSA and Pr(III) complex.

3.2.2. Binding constant and binding sites

The apparent binding constant K_A and binding sites n can be evaluated using the following equation (Eq. (2)) [45].

$$\log \frac{F_0 - F}{F} = n \log K_A - n \log \left\{ \frac{1}{[D_t] - (F_0 - F)[P_t]/F_0} \right\} \quad (2)$$

where F_0 and F are the fluorescence intensities before and after the addition of the quencher, respectively, and $[D_t]$ and $[P_t]$ are the total quencher concentration and the total protein concentration, respectively. Based on the plot of $\log(F_0 - F)/F$ versus $\log(1/([D_t] - (F_0 - F)[P_t]/F_0))$ (see Supporting Information Fig. S2), the number of binding sites n and binding constant K_A can be obtained, as presented in Table 2. It was noticed that the binding constant values decreased with increase in temperature due to reduction of the stability of Pr(III) complex–BSA system. The value of n is helpful to know the number of binding sites and to locate the binding site in BSA for the drug, which was noticed to be almost unity indicating that there was one independent class of binding site on BSA for complex.

3.2.3. Main binding force between complexes and BSA

The interaction force between compounds and proteins pertains to weak interaction, including hydrogen bond, hydrophobic force, electrostatic force, and Van der Waals' interaction. If $\Delta H \approx 0$, $\Delta S > 0$, the main force is hydrophobic interaction; if $\Delta H < 0$, $\Delta S > 0$, the main force is electrostatic effect; if $\Delta H < 0$, $\Delta S < 0$, Van der Waals and hydrogen bond interactions play major role in the reaction [46]. The enthalpy change ΔH and entropy change ΔS for a binding reaction can be derived from the vant't Hoff equations (Eq. (3)).

$$\ln K_A = -\frac{\Delta H}{RT} + \frac{\Delta S}{R} \quad (3)$$

where K_A is analogous to the binding constant at the corresponding temperature, R is gas constant. The free energy change can be obtained from the following relationship (Eq. (4)).

$$\Delta G = \Delta H - T\Delta S \quad (4)$$

Using the above two equations the values of ΔG, ΔH, ΔS were obtained and shown in Table 2. The binding process was always spontaneous as demonstrated by the negative value of ΔG and the formation of the Pr(III) complex–BSA is an exothermic process, accompanied by negative enthalpy and positive entropy changes. Positive ΔH and ΔS values are frequently taken as typical evidence of hydrophobic interactions, while negative enthalpy and entropy changes arise from van der Waals and hydrogen bonding formation [47,46]. Therefore from these results, the binding of Pr(III) complex to BAS appears to involve hydrophobic interactions as shown by the positive value of ΔS although a lower component of electrostatic interactions cannot be excluded.

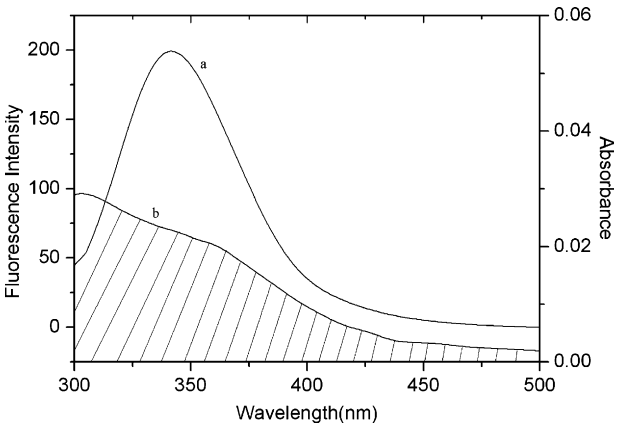

Fig. 5. Overlap of fluorescence spectra of BSA and UV absorption spectrum of Pr(III) complex. (a) Fluorescence spectra of BSA (1.50×10^{-6} M); (b) UV absorption spectrum of Pr(III) complex (1.50×10^{-6} M).

3.2.4. Energy transfer from BSA to complexes

According to Förster nonradiative energy-transfer theory [48], the efficiency of energy transfer is E, the critical distance for 50% energy transfer is R_0, and the actual distance of separation is r. These values were calculated by Eqs. (5) and (6).

$$E = 1 - \frac{F}{F_0} = \frac{R_0^6}{R_0^6 + r^6} \quad (5)$$

$$R_0^6 = 8.78 \times 10^{-25} \kappa^2 n^{-4} \Phi_{Trp} J \quad (6)$$

where κ^2 is the orientation factor, Φ_{Trp} is the quantum yield of the donor tryptophan in the absence of acceptor, n is the refractive index of the medium intervening between the donor and acceptor, and J is the spectral overlap integral defined by Eq. (7).

$$J = \frac{\sum F(\nu)\varepsilon(\nu)\nu^{-4}\Delta\nu}{\sum F(\nu)\Delta\nu} \quad (7)$$

where $F(\nu)$ is the fluorescence intensity of the donor, $\varepsilon(\nu)$ is the molar extinction coefficient of the acceptor in units of M^{-1} cm^{-1}, and ν is the frequency in cm^{-1}. The fluorescence emission spectrum of BSA and the UV-absorption spectrum of the Pr(III) complex was shown in Fig. 5, which reveals that they have some overlap. The value of J was 1.98×10^{14} cm^3 l M^{-1} for the complex. The orientation factor, κ^2 taken as 2/3 and the refractive index, n, was taken as 1.36 [48]. The quantum yield, Φ_{Trp}, was determined in the study as 0.15 [49]. With use of the values of J, κ^2, n and Φ_{Trp}, R_0 value was calculated as 2.86 nm for the Pr(III) complex. The E was 0.08357 for the complex, so the energy transfer efficiency from BSA to the Pr(III) complex is very weak. The actual distance r, between the binding site of complexes binding in BSA molecule and Trp212 in BSA polypeptide chain was 4.26 nm for its Pr(III) complex. The average distance of 2–8 nm between a donor and acceptor indicated that the energy transfer from BSA to complexes occurred with high probability [50].

3.2.5. Changes of BSA's secondary structures induced by complexes binding

Further experiments were carried out with CD technique to verify the binding of complexes to BSA. As Fig. 6 shows, a CD spectrum of BSA gives double negative peaks, and the peak at 208 nm is higher than the peak at 222 nm. When the complex added in BSA, the intensity of the two bands increased, clearly indicating the increase of the a-helical content in protein, respectively [51]. The average fractions of secondary structure estimated from the CD data are given in Table 3. The regular α-helix content was 42.27% and the distorted α-helix content was 14.57% in the BSA, while the reg-

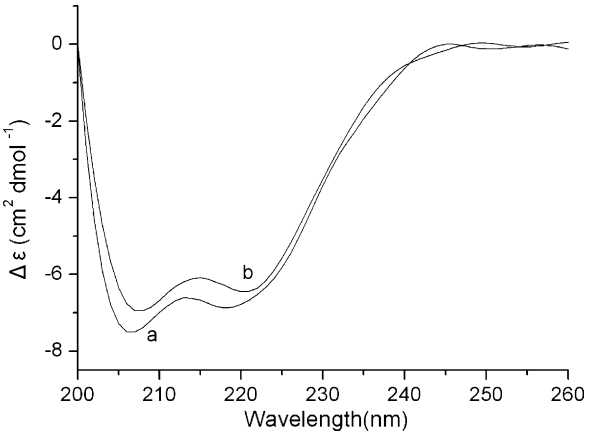

Fig. 6. CD spectra of the BSA–Pr(III) complex system. (a) 1.50×10^{-6} M BSA; (b) 1.50×10^{-6} M BSA + 1.50×10^{-6} M Pr(III) complex.

ular α-helix structure were reduced to 37.20% and the distorted α-helix structure increase to 23.50%, when the complex bind to BSA. Moreover, the binding of this complex to BSA arouse the increase of the regular β-strand content and turn, the decrease of distorted β-strand content and unordered structure. The calculated results still exhibited a reduction of α-helix structure from 56.84% to 50.2% for Pr(III) complex, as described in Fig. 6. All the results indicate that the binding of Pr(III) complex to BSA induces a conformational change in BSA.

3.3. DNA binding studies

3.3.1. Electronic absorption titration

The UV–Vis absorption spectra of the investigated compounds in the absence and in the presence of the CT DNA were obtained in DMF:Tris–HCl buffer (5 mmol, pH 7.20) containing 50 mmol NaCl of 1:100 solutions, respectively (see Supporting Information Fig. S3). In the UV spectrum of ligand, the intensity of the bands centered at 300 nm and 356 nm decreased in the presence of increasing amounts of CT DNA. For its Pr(III) complex, the absorption bands at 305 nm and 363 nm exhibited hypochromism of about 46.82 and 48.21%, with no shifts in the region of 305–363 nm. The observed hypochromism could be attributed to stacking interaction between the aromatic chromophore of the complexes and DNA base pairs consistent with the intercalative binding mode [52].

The results derived from the UV titration experiments suggest that all compounds bind to DNA although the exact mode of binding cannot be merely proposed by UV spectroscopic titration studies. Nevertheless, the ofloxacin ligand provides an aromatic/planar moiety so that the binding of the complex involving intercalation between the base pairs of CT DNA cannot be ruled out.

The binding constant K_b is a useful tool in order to calculate the magnitude of the binding strength of compounds with CT DNA and represents the binding constant per DNA base pair. It was usually determined using the following equation (Eq. (8)) [53].

$$\frac{[\mathrm{DNA}]}{(\varepsilon_a - \varepsilon_f)} = \frac{[\mathrm{DNA}]}{(\varepsilon_b - \varepsilon_f + 1/K_b(\varepsilon_b - \varepsilon_f))} \quad (8)$$

Table 3
Average estimates of the secondary structure fractions of BSA solutions obtained with the CDPro software package after reaction with $[PrL_2(NO_3)](NO_3)_2$.

Compound	Fraction of secondary structure (%)					
	α_R	α_D	β_R	β_D	T	U
BSA	42.27	14.57	3.13	12.23	7.00	21.13
BSA + $[PrL_2(NO_3)](NO_3)_2$	26.70	23.50	7.40	11.60	15.27	11.40

where [DNA] is the concentration of DNA in base pairs, ε_a corresponds to the extinction coefficient observed (A_{obsd}/[M]), ε_f corresponds to the extinction coefficient of the free compound, ε_b is the extinction coefficient of the compound when fully bound to DNA, and K_b is the intrinsic binding constant. The ratio of slope to intercept in the plot of [DNA]/($\varepsilon_a - \varepsilon_f$) versus [DNA] gives the values of K_b [54].

The values of K_b are 5.17×10^3 M^{-1} and 1.01×10^4 M^{-1} for the ligand and its Pr(III)complex. The K_b values of the complex are higher than that of ligand suggesting that ligand presents higher affinity to CT DNA, when it is coordinated to Pr(III). The higher binding affinity of the Pr(III) complex is probably attributed to the extension of the π system of the intercalated ligand, which leads to a planar area greater than that of the free ligand, so the coordinated ligand penetrates more deeply into and stacks more strongly with DNA base pairs.

3.3.2. EB–DNA quenching assay

The DNA binding modes of the compounds were also monitored by a fluorescent EB displacement assay. EB is a phenanthridine fluorescence dye and is a typical indicator of intercalation, forming soluble complexes with nucleic acids and emitting intense fluorescence in the presence of CT DNA due to the intercalation of the planar phenanthridinium ring between adjacent base pairs on the double helix [55].

The emission spectra of EB bound to CT DNA in the absence and presence of each compound have been recorded for [EB] = 0.32 μM, [DNA] = 4 μM for increasing amounts of each compound. The addition of the Pr(III) complex to the DNA-bound EB solutions caused marked reduction in emission intensities, however, the addition of the ligand arouse little reduction in intensities (see Supporting Information Fig. S4). The observed quenching of DNA–EB fluorescence from Pr(III) complex suggests that the complex can moderately displace EB from the DNA–EB complex and it can probably interact with CT DNA by the intercalative mode [56,57], but for the ligand, the external contact may not excluded.

The quenching plots illustrate that the quenching of EB bound to DNA by the compounds which are in good agreement with the linear Stern–Volmer equation (Eq. (1)). In the plots of F_0/F versus [Q], K_{SV} is given by the ratio of the slope to the intercept. The data show that the interaction of the Pr(III) complexes (2.78×10^4 M^{-1}) with DNA is stronger than that of the free ligand(1.11×10^3 M^{-1}), which is consistent with the electronic absorption spectral results.

3.3.3. KI quenching

KI can effectively quench the fluorescence of a small molecule, and the interaction mode of the small molecule with DNA can be deduced from the variation of the fluorescence in the absence and presence of DNA. When small molecule intercalates to DNA base pairs, owing to the electrostatic repelling between DNA phosphate backbone and the iodide anions, the iodide anions are difficult to collide with the small molecules, which lead to a decrease in fluorescent quenching [58]. On the contrary, surface-binding mode between small molecule and DNA cannot afford a protection surrounding for the small molecule, the collision probability between small molecule and iodide anions with the presence and absence of DNA will be equal. When the interaction mode belongs to groove binding, the small molecules will be partly protected by DNA, and iodide anions can partly quench its fluorescence [59,60].

From the results of the emission titrations for the Pr(III) complex and potassium iodide with absence and presence of CT DNA, we can found that the iodide anions could quench the fluorescence of complex–DNA system and the solution that only contains complex. The quenching data were plotted according to the Stern–Volmer equation (Eq. (1)) and the slopes were calculated by the linear least-squares method. The observed quenching constants were 5.02 M^{-1}

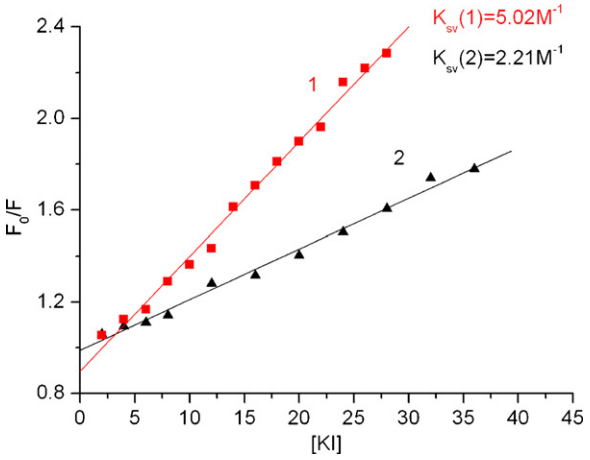

Fig. 7. Stern–Volmer plot of the fluorescence titration data of Pr(III) complex. Effect of KI concentration (1: Pr(III) complex + KI; 2: Pr(III) complex + KI + CT DNA).

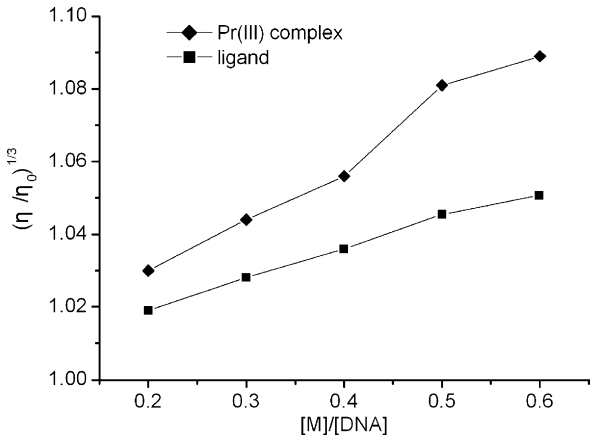

Fig. 9. Effect of increasing amounts of the ligand and Pr(III) complex on the relative viscosity of CT DNA at 25.0 °C.

and 2.21 M^{-1} with and without CT DNA for the Pr(III) complex (Fig. 7). The quenching of the complex was in fact enhanced by a factor of approach 2 when the complex was bound to the DNA helix. We can conclude that the complexes are intercalated into the DNA helix and they should be protected from the anionic quencher, owning to the base pairs above and below the intercalators [61].

3.3.4. Salt effect

The effect of the ionic strength on the complexes fluorescence intensity was tested by the addition of a strong electrolyte, such as NaCl, instead of potassium iodide. Cations of the salts can neutralize the negatively charged phosphate. If the compound binds to DNA through an electrostatic interaction mode, the surface of DNA will be surrounded by the sodium ions with the increase of ionic strength. Then the compound is difficult to approach DNA and the strength of interaction with DNA decreases, the degree of fluorescence quenching also falls [62]. As seen from Fig. 8, addition of NaCl to the complexes in the absence and presence of CT DNA has little or no influence on the fluorescence intensity, showing that the interaction of the complexes with CT DNA is not electrostatic interaction.

3.3.5. Viscosity titration measurements

To further clarify the interactions between the studied compounds and CT DNA, viscosity measurements were carried out. Measurements of DNA viscosity that is sensitive to DNA length are regarded as the least ambiguous and the most critical tests of binding in solution in the absence of crystallographic structural data [63,64]. A classical intercalation mode demands that the DNA helix must lengthen as base pairs are separated to accommodate the binding complexes, leading to the increase of DNA viscosity, as for the behaviors of the known DNA intercalators [65]. In contrast, a partial and/or non-classical intercalation of the complex could bend (or kink) the DNA helix, reducing its viscosity concomitantly [66]. The effects of all the compounds on the viscosity of CT DNA are shown in Fig. 9. The viscosities of the DNA increase steadily with increasing concentrations of ligand and the Pr(III) complex, and the extent of the increase observed for the ligand is smaller than that for the Pr(III) complexes. Viscosity measurements clearly show that all the compounds can intercalate between adjacent DNA base pairs, causing an extension in the helix and thus increase the viscosity of DNA, and that the complex can intercalate more strongly and deeply than the free ligand. The results obtained from the viscosity experiments validate those obtained from the spectroscopic studies.

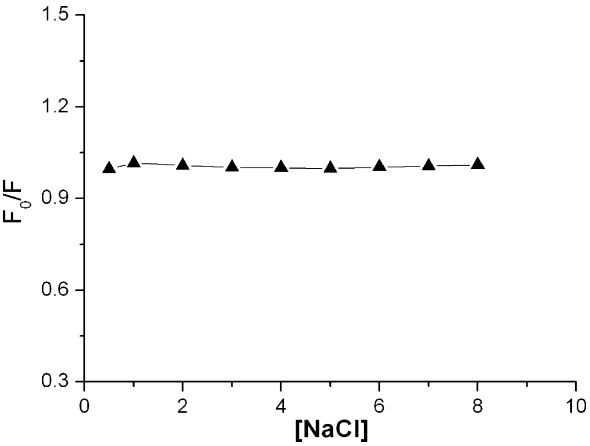

Fig. 8. Effect of NaCl concentration (Pr(III) complex + NaCl + CT DNA).

3.4. Cleavage plasmid pBR322 DNA

3.4.1. Chemical nuclease activity

In order to assess the chemical nuclease activities of the Pr(III) complexes for DNA strand scission, pBR322 DNA was incubated with the Pr(III) complex under the reaction conditions. The cleavage reaction can be monitored by gel electrophoresis. When circular pBR322 DNA is subjected to electrophoresis, relatively fast migration will be observed for the intact supercoiled form (Form I). If scission occurs on one strand (nicking), the supercoiled form will relax to generate a slower-moving nicked form (Form II). If both strands are cleaved, a linear form (Form III) that migrates between Form I and Form II will be generated [67,68].

To assess the DNA cleavage ability of the complexes, supercoiled pBR322 DNA (20 μM) was incubated with 20–100 μM of the Pr(III) complex in TBE buffer for 5 h without the addition of a reductant [69]. Control experiments show that the free ligand and $Pr(NO_3)_3{\cdot}6H_2O$ are cleavage inactive (Fig. 10). The SC DNA (form I) was cleaved by the complex, especially when the concentration of the complex is 60 μM (Fig. 11). At the concentration of 60 μM, the Pr(III) complex can almost promote the complete conversion of plasmid pBR 322 from Form I to Form II (lane 4). However, the cleavage activity decreased when the concentration of the complex went on increasing. The result indicates that the cleavage efficiency depends on the concentration of complex.

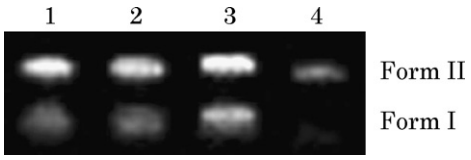

Fig. 10. Agarose gel electrophoresis patterns for the cleavage reaction of the pBR 322 DNA with 60 μM of free ligand and free $Pr(NO_3)_3{\cdot}6H_2O$ for 5 h at 37 °C in a TBE buffer at pH 8.3. Lane 1: pure DNA, without any additives; lane 2: DNA + 60 μM of $Pr(NO_3)_3{\cdot}6H_2O$; lane 3: DNA + 60 μM of ligand; lane 4: DNA + 60 μM of Pr(III) complex.

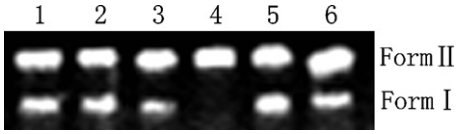

Fig. 11. Agarose gel electrophoresis of the cleavage of the pBR 322 DNA in the absence (lane 1) and in the presence of Pr(III) complex at various concentrations for 5 h at 37 °C in a TBE buffer at pH 8.3. Lane 1: DNA control; lanes 2–6: DNA + [complex] = 20, 40, 60, 80, 100 μM, respectively.

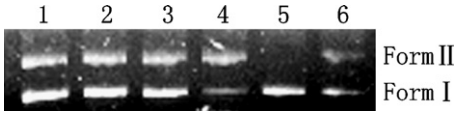

Fig. 12. Agarose gel showing cleavage of pBR322 DNA (0.1 μg/μL) incubated with 0.1 mM Pr(III) complexes for 5 h. at 37 °C in TBE buffer at pH 8.3. Lane 1: DNA control; lane 2: DNA + Pr(III) complex; lane 3: DNA + Pr(III) complex + 100 mM NaN_3; lane 4: DNA + Pr(III) complex + 100 mM L-Histidine; lane 5: DNA + Pr(III) complex + 2 μL DMSO; lane 6: DNA + Pr(III) complex + 2 μL EtOH.

3.4.2. Mechanistic studies

The DNA cleavage activity of the complexes has been studied in the presence of several additives to understand the mechanistic pathway involved in the DNA cleavage reaction (Fig. 12). From Fig. 12, we can see that no obvious inhibitions are observed for the Pr(III) complex in the presence of NaN_3 (lane 3) and L-Histidine (lane 4), the results rule out the possibility of DNA cleavage by the singlet oxygen or a singlet oxygen-like entity. The addition of DMSO (lane 5), EtOH (lane 6) partly diminishes the nuclease activity of the Pr(III) complex which is indicative of the involvement of hydroxyl radical in the cleavage process.

4. Conclusions

The Pr(III) complex are prepared from $Pr(NO_3)_3{\cdot}6H_2O$ and acylhydrazone ligands derived from ofloxacin. Firstly, the interaction between the Pr(III) complex and BSA has been investigated by fluorescence method combined with UV–Vis and CD spectroscopy techniques under simulative physiological conditions. The results showed that the intrinsic fluorescence of BSA was quenched through static quenching mechanism and the Pr(III) complex bound to BSA with high affinity which is predominantly owing to hydrophobic and electrostatic effect. The Pr(III) complex can be deposited and transported by albumin. Experimental results also showed that the binding of the Pr(III) complex to BSA induced a conformational change of BSA, which was further proved by the quantitative analysis data of CD spectrum. Secondly, the DNA binding mode of Pr(III) complex and ligand with CT DNA were also studied via spectra and viscosity measurement. The results indicate that the Pr(III) complex bind to DNA via an intercalation mode and the Pr(III) complex can bind to DNA more strongly than the free ligand. Noticeably, the Pr(III) complex has been found to promote cleavage of plasmid pBR 322 DNA. Results obtained from our present work would be useful to understand the mechanism of interactions of the small molecule compounds binding to BSA and DNA, and helpful in the development of their potential biological, pharmaceutical and physiological implications in the future.

Appendix A. Supplementary data

Supplementary data associated with this article can be found, in the online version, at doi:10.1016/j.saa.2010.11.018.

References

[1] A. Datta, N.K. Karan, S. Mitra, V.J. Gramlich, J. Chem. Crystallogr. 33 (2003) 579–583.
[2] B. Gillon, C. Mathoniere, E. Ruiz, S. Alvarez, A. Cousson, T.M. Kahn, J. Am. Chem. Soc. 124 (2002) 14433–14441.
[3] D.C. Carter, J.X. Ho, Adv. Protein Chem. 45 (1994) 153–203.
[4] F. Zsila, Z. Bikadi, M. Simonyi, Biochem. Pharmacol. 65 (2003) 447–456.
[5] Y.B. Zeng, N. Yang, W.S. Liu, N. Tang, J. Inorg. Biochem. 97 (2003) 258–264.
[6] A.E. Friedman, C.V. Kumar, N.J. Turro, J.K. Barton, Nucleic Acids Res. 19 (1991) 2595–2602.
[7] A.M. Pyle, T. Morii, J.K. Barton, J. Am. Chem. Soc. 112 (1990) 9432–9434.
[8] D.C. Cater, J.X. Ho, Adv. Protein Chem. 45 (1994) 153–203.
[9] S. Curry, P. Brick, N.P. Frank, Biochim. Biophys. A 1141 (1991) 131–140.
[10] Y.M. Wang, Y. Song, D.L. Kong, Chin. Sci. Bull. 50 (2005) 1839–1844.
[11] R.K. Mehra, K. Tran, G.W. Scott, P. Mulchandani, S.S. Saini, J. Inorg. Biochem. 61 (1996) 125–142.
[12] Y.B. Battal, M. Topuzogullari, Z. Mustafaeva, J. Fluoresc., doi:10.1007/s10895-009-0484-9.
[13] A.R.A. Abd-Allah, B.B. Gannam, F.M.A. Hamada, Pharm. Res. 42 (2000) 145–150.
[14] W.E. Sanders Jr., Clin. Infect. Dis 14 (1992) 539–554.
[15] K.C. Skyrianou, E.K. Efthimiadou, V. Psycharis, A. Terzis, D.P. Kessissoglou, G. Psomas, J. Inorg. Biochem. 103 (2009) 1617–1625.
[16] K.C. Skyrianou, F. Perdih, I. Turel, D.P. Kessissoglou, G. Psomas, J. Inorg. Biochem. 104 (2010) 161–170.
[17] A. Tarushi, C.P. Raptopoulou, V. Psycharis, A. Terzis, G. Psomas, D.P. Kessissoglou, Bioorg. Med. Chem. 18 (2010) 2678–2685.
[18] R.T. Mostafa, H.M. Seyed, R. Bijan, Biochem. Mol. Biol. Int. 39 (2006) 530–536.
[19] S. Zahra, H. Saman, R. Bijan, N.G. Mohsen, Biochem. Mol. Biol. Int. 39 (2006) 636–641.
[20] N. Sreerama, R.W. Woody, Anal. Biochem. 287 (2000) 252–260.
[21] N.J. Greenfield, Anal. Biochem. 235 (1995) 1–10.
[22] N. Sreerama, R.W. Woody, Anal. Biochem. 209 (1993) 32–44.
[23] J.Y. Zheng, A.C. Celeste, K.R. Vipin, T.C. Cheng, J.D. Joseph, M.L. Roger, J. Phys. Chem. B 108 (2004) 17238–17242.
[24] A.V. Milyutin, L.R. Amirova, V.E. Kolla, F.Y. Nazmetdinov, L.P. Drovosekova, Y.S. Andreichikov, Pharm. Chem. J. 32 (1998) 422–424.
[25] P.X. Xi, Z.H. Xu, F.J. Chen, Z.Z. Zeng, X.W. Zhang, J. Inorg. Biochem. 103 (2009) 210–218.
[26] F.J. Chen, G.Q. Liu, Z.H. Xu, Z.Z. Zeng, Biochem. Mol. Biol. Int. 41 (2008) 305–309.
[27] M. Eriksson, M. Leijon, C. Hiort, B. Norden, A. Gradsland, Biochemistry 33 (1994) 5031–5040.
[28] Y. Xiong, X.F. He, X.H. Zou, J.Z. Wu, X.M. Chen, L.N. Ji, R.H. Li, J.Y. Zhou, R.B. Yu, J. Chem. Soc., Dalton Trans. 1 (1999) 19–24.
[29] W.J. Geary, Coord. Chem. Rev. 7 (1971) 81–122.
[30] F.D. Lewis, S.V. Barancyk, J. Am. Chem. Soc. 111 (1989) 8653–8661.
[31] N. Raman, A. Kulandaisamy, K. Jeyasubramanian, J. Ind. Chem. 41A (2002) 942–949.
[32] B.D. Wang, Z.Y. Yang, D.W. Zhang, Y. Wang, Spectrochim. Acta Part A 63 (2006) 213–219.
[33] M.M. Moawad, W.G. Hanna, J. Coord. Chem. 55 (2002) 439–457.
[34] T.M.A. Ismail, J. Coord. Chem. 58 (2005) 141–151.
[35] J.R. Lakowicz, Principles of Fluorescence Spectroscopy, second ed. Plenum, New York, 1999.
[36] I. Sjoholm, B. Ekman, A. Kober, I. Ljungstedt-Pahlman, B. Seiving, T. Sjodin, Mol. Pharmacol. 16 (1979) 767–777.
[37] S.S. Lehrer, Biochemistry 10 (1971) 3254–3263.
[38] J.R. Lakowicz, G. Weber, Biochemistry 12 (1973) 4161–4170.
[39] C.Q. Jiang, M.X. Gao, J.X. He, Anal. Chim. Acta 452 (2002) 185–189.
[40] Y.M. Huang, Z.J. Zhang, D.J. Zhang, Talanta 53 (2001) 835–841.
[41] L.H. Qian, X.L. Wang, Z.H. Tu, Acta Pharmacol. Sin. 22 (2001) 847–850.
[42] P. Das, A. Mallick, B. Haldar, A. Chakrabarty, N. Chattopadhyay, J. Chem. Phys. 125 (2006), 044516/1–6.
[43] A. Mallick, B. Haldar, N. Chattopadhyay, J. Phys. Chem. B 109 (2005) 14683–14690.
[44] M. Bardhan, G. Mandal, T. Ganguly, J. Appl. Phys. 106 (2009) 034701–034705.
[45] S.Y. Bi, L. Ding, Y. Tian, D.Q. Song, X. Zhou, H.Q. Zhang, J. Mol. Struct. 703 (2004) 37–45.
[46] P.D. Ross, S. Subramanian, Biochemistry 20 (1981) 3096–3102.
[47] S.N. Timaseff, in: H. Peeters (Ed.), Proteins of Biological Fluids, Pergamon Press, Oxford, 1972, pp. 511–519.
[48] W. De, W. Horrocks, W.E. Collier, J. Am. Chem. Soc. 103 (1981) 2856–2862.
[49] X.H. Liu, X.P. Xian, F.J. Chen, Z.H. Xu, Z.Z. Zeng, J. Photochem. Photobiol. B 92 (2008) 98–102.

[50] Y.J. Hu, Y. Liu, L.X. Zhang, J. Mol. Struct. 750 (2005) 174–178.
[51] Y.H. Chen, J.T. Yang, H.M. Martinez, Biochemistry 11 (1972) 4120–4131.
[52] A.M. Pyle, J.P. Rehmann, R. Meshoyrer, C.V. Kumar, N.J. Turro, J.K. Barton, J. Am. Chem. Soc. 111 (1989) 3053–3063.
[53] A. Wolf, G.H. Shimer, T. Meehan, Biochemistry 26 (1987) 6392–6396.
[54] S. Bhattacharya, G. Mandal, T. Ganguly, J. Photochem. Photobiol. B: Biol. 101 (2010) 89–96.
[55] G. Zhao, H. Lin, S. Zhu, H. Sun, Y. Chen, J. Inorg. Biochem. 70 (1998) 219–226.
[56] G. Psomas, A. Tarushi, E.K. Efthimiadou, Polyhedron 27 (2008) 133–138.
[57] O. Novakova, H. Chen, O. Vrana, A. Rodger, P.J. Sadler, V. Brabec, Biochemistry 42 (2003) 11544–11554.
[58] X. Yang, W.H. Liu, W.J. Jin, G.L. Shen, R.Q. Yu, Spectrochim. Acta Part A 55 (1999) 2719–2727.
[59] C.V. Kumar, E.H. Asuncion, J. Chem. Soc. Chem. Commun. 6 (1992) 470–472.
[60] C.V. Kumar, R.S. Turner, E.H. Asuncion, J. Photochem. Photobiol. A: Chem. 74 (1993) 231–238.
[61] L.S. Lerman, J. Mol. Biol. 3 (1961) 18–30.
[62] G.M. Howe, K.C. Wu, W.R. Bauer, Biochemistry 15 (1976) 4339–4346.
[63] S. Mahadevan, M. Palaniandavar, Inorg. Chem. 37 (1998) 693–700.
[64] A.B. Tossi, J.M. Kelly, Photochem. Photobiol. 9 (1989) 545–556.
[65] J.G. Liu, Q.L. Zhang, X.F. Shi, L.N. Ji, Inorg. Chem. 40 (2001) 5045–5050.
[66] S. Satyanarayana, J.C. Dabrowiak, J.B. Chaires, Biochemistry 32 (1993) 2573–2584.
[67] X.W. Liu, J. Li, H. Li, K.C. Zheng, H. Chao, L.N. Ji, J. Inorg. Biochem. 100 (2006) 385–395.
[68] H. Chao, W.J. Mei, Q.W. Huang, L.N. Ji, J. Inorg. Biochem. 92 (2002) 165–170.
[69] M.S. Deshpande, A.A. Kumbhar, A.S. Kumbhar, M. Kumbhakar, H. Pal, U.B. Sonawane, R.R. Joshi, Bioconjugate Chem. 20 (2009) 447–459.